ORIGINAL ARTICLE

International Journal of Applied Mathematics in Control Engineering

Journal homepage: http://www.ijamce.com

Study on Structural Evolution and Properties of Fluorinated Graphene Regulated by Fluorination Degree

Lifen Liang[1]* | Longjie Miao[1] | Shenghang Ma[1] | Xiurong Sun[1]

[1]Hebei University of Environmental Engineering, Qinhuangdao 066102, Hebei, China

Correspondence
Hebei University of Environmental Engineering, Qinhuangdao 066102, Hebei, China
Email: lianglifen@hebuee.cn

Article Info
Article history:
Received 12 March 2025
Accepted 21 May 2025
Available online 22 May 2025

Abstract

In this study, graphene was prepared from natural flake graphite via secondary chemical intercalation, microwave expansion, and liquid-phase reduction. Fluorinated graphene with different fluorine-to-carbon (F/C) ratios was then synthesized at various temperatures using direct gas fluorination. Characterizations by SEM, AFM, BET, XPS, and TGA showed that as the fluorination degree increased (F/C ratio from 0.344 to 1.045), the average particle size and layer number of fluorinated graphene flakes decreased, the specific surface area increased, and the C-F bonding transformed from semi-ionic to covalent bonds, significantly enhancing thermal stability. This study reveals the regulatory mechanism of fluorination degree on the structure and properties of fluorinated graphene (FG), providing a theoretical basis for its wide applications.

KEYWORDS

Graphene, Fluorinated graphene, Fluorine-to-carbon ratio, Gas fluorination method, Performance characterization

1 | INTRODUCTION

Fluorinated graphene (FG) is a novel graphene derivative that retains graphene's layered structure, featuring a high specific surface area, excellent structural properties, and mechanical performance. The introduction of fluorine atoms reduces graphene's surface energy, enhances hydrophobicity, and improves thermal stability, chemical stability, and lubricity [1, 2], endowing it with potential applications in nanoelectronic devices, lubricating coatings, and energy storage [3, 4, 5, 6]. Its properties are highly dependent on the fluorination degree (F/C ratio) and the type of C-F bonding (semi-ionic or covalent). Thus, preparing fluorinated graphene with different fluorination degrees and systematically characterizing its properties is crucial for expanding its applications.

Fluorinated graphene was first synthesized by Nair [7] and Zboři [8] in 2010 through graphene fluorination and mechanical exfoliation of fluorinated graphite, respectively. Currently, its preparation methods are mainly categorized into fluorination and exfoliation methods. The direct fluorination method, with advantages of high efficiency, low cost, and structural controllability, has become the most industrially promising route. However, it faces challenges in practical operation: low reactivity of raw materials at low temperatures leads to low fluorination degrees, difficulty in coordinating flake size with fluorination degree, and poor uniformity. In recent years, researchers have improved the direct fluorination method by introducing pretreatment steps

Digital Object Identifiers: 10.62953/IJAMCE.703824

and optimizing reaction conditions [9, 10, 11, 12]. For example, Wang [13] used commercial fluorine/nitrogen gas mixtures for in-situ direct fluorination of industrially produced graphene oxide (GO) at low temperatures, successfully preparing fluorinated graphene with varying F/C ratios while maintaining large flake structures and thermal stability up to 400 °C, providing valuable insights for method optimization. The exfoliation method avoids toxic fluorine sources and can be operated in laboratories without special equipment but suffers from low efficiency and yield. Scholars have used solvent-assisted ultrasonic chemical exfoliation and thermal exfoliation [14, 15, 16, 17] to adjust FG's fluorine content by altering intercalants, ultrasonic power, and time, yet controlling the number of layers remains challenging, with low yields of single-layer and few-layer FG.

Despite progress in FG preparation and property research, issues persist. On one hand, process optimization needs further exploration to achieve higher-quality, more stable production. On the other hand, systematic studies on correlations between FG's microstructure, surface properties, and thermal stability under different fluorination degrees are insufficient. This study aims to integrate improved preparation methods and advanced characterization techniques to clarify the preparation-structure-performance relationship of FG, laying a foundation for its multi-field applications.

Using natural flake graphite as the raw material, this study prepares nanoscale graphene flakes via the redox method and synthesizes fluorinated graphene with different F/C ratios (FG-0.3, FG-0.5, FG-0.8, and FG-1) by direct gas fluorination. SEM, AFM, specific surface area analysis, XPS, and TGA are used to systematically characterize FG's microstructure, chemical composition, and thermal stability, revealing the influence of fluorination degree on FG's chemical composition and properties, thus providing experimental and theoretical support for its applications.

2 | MATERIALS

The materials used in this study include: natural flake graphite (specification: LG150-99) from Qingdao Tianheda Graphite Co., Ltd., Shandong Province; 72 wt% perchloric acid, analytical grade potassium permanganate, iron powder (purity: 98%, 400 mesh), and 35 wt% hydrochloric acid, all supplied by Tianjin Kemiou Chemical Reagent Co., Ltd.; and analytical grade anhydrous ethanol from Tianjin No.3 Chemical Reagent Factory.

3 | PREPARATION OF FLUORINATED GRAPHENE

3.1 | Preparation of Graphene

The preparation process of graphene is shown in Figure 1. Using natural flake graphite as the raw material, perchloric acid as the intercalant, and potassium permanganate as the oxidant, a primary intercalation reaction was carried out. The specific process was as follows: 1 g of natural flake graphite and 0.38~0.42 g of potassium permanganate were placed in a beaker, which was then placed on a multi-functional magnetic stirrer; 9.5~10.5 g of perchloric acid was added to the beaker; the magnetic stirrer with the beaker was placed in a fume hood, and the stirrer was turned on to stir the mixed solution for the primary intercalation reaction of flake graphite. The temperature of the mixed solution was controlled at 40~50 °C, and the reaction time was 50~60 min. After the primary intercalation reaction, the mixed solution was filtered to collect the retained solid, which was fully washed with deionized water until the pH of the washing water was neutral. The washed solid was then freeze-dried at -40 °C for 15 h to obtain expandable graphite after primary intercalation. 4~6 g of the primary intercalated expandable graphite was placed in a microwave oven with a power of 900 W for microwave expansion treatment, with a microwave expansion time of 20~25 s. After microwave expansion, the average expansion ratio of the expandable graphite was 250 mL/g, which was recorded as primary expanded graphite.

Then, the primary expanded graphite was subjected to secondary chemical intercalation and secondary expansion using the same method as above to obtain secondary expanded graphite. 50 mg of secondary expanded graphite powder was placed in a beaker containing 30 mL of deionized water, and the beaker was then placed in an ultrasonic processor for ultrasonic treatment. The ultrasonic frequency was 40 kHz, the ultrasonic water bath temperature was 20~30 °C, and the ultrasonic dispersion time was 30~60 min, obtaining a graphene oxide ultrasonic dispersion. Subsequently, liquid-phase reduction was performed using Fe

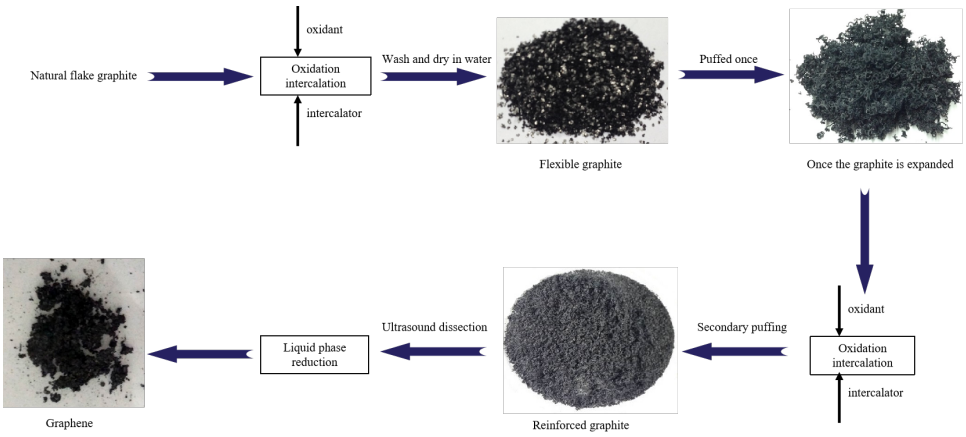

FIGURE 1 Schematic diagram for preparation process of graphene.

powder and hydrochloric acid (1 g of iron powder, 20 mL of 35% hydrochloric acid, reaction for 30 min). After liquid-phase reduction, the sample was washed with water to neutrality and freeze-dried to obtain graphene powder.

3.2 | Preparation of Fluorinated Graphene

Fluorinated graphene with different fluorine-to-carbon ratios was prepared by the direct gas fluorination method. As shown in Figure 2, a certain amount of graphene raw material was weighed into a porcelain boat, spread evenly with the powder stacking thickness less than 1 cm, and placed in the tube of a vacuum tube furnace. The tube was evacuated to a vacuum degree of -0.01 MPa. Then, the temperature of the tube furnace chamber was raised to 200 °C at a heating rate of 5 °C/min and maintained for 2 hours to remove residual moisture in the graphene sheets. After the furnace chamber temperature naturally cooled to room temperature, a mixed gas of fluorine and nitrogen (with fluorine accounting for 20% by volume) was continuously introduced, and the temperature was raised to 370-450 °C at a heating rate of 5 °C/min for a fluorination reaction lasting 10 hours. After the reaction, fluorinated graphene with different fluorination degrees was obtained, denoted as FG-0.3, FG-0.5, FG-0.8, and FG-1. Their fluorine content and fluorine-to-carbon ratio were analyzed in the subsequent XPS test. Among them, the reaction temperatures corresponding to FG-0.3, FG-0.5, FG-0.8, and FG-1 are 370 °C, 400 °C, 420 °C, and 450 °C respectively. It can be seen from the figure that as the fluorination degree increases, the color of fluorinated graphene gradually changes from the black of original graphene to white.

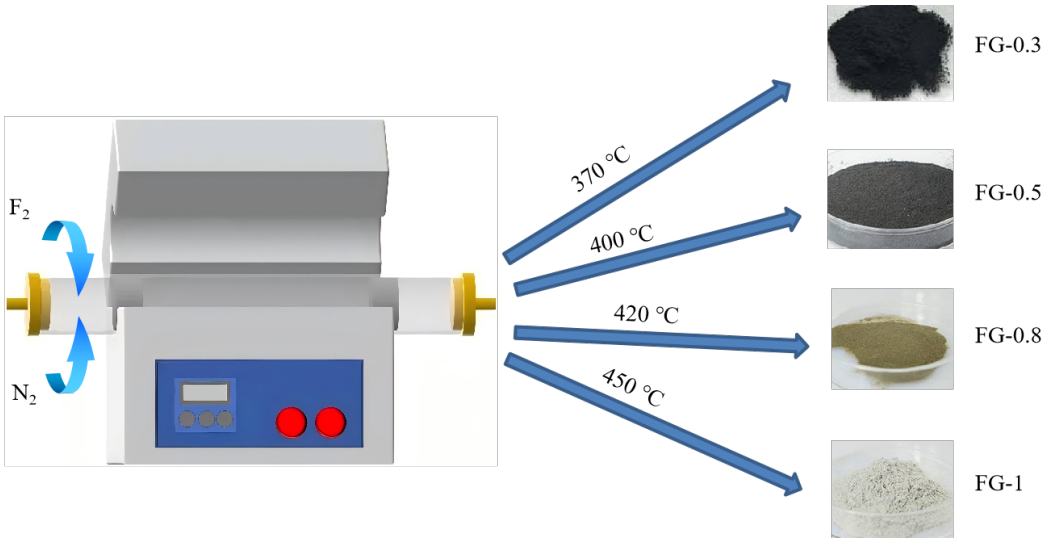

FIGURE 2 Schematic diagram for preparation process of fluorinated graphene.

4 | ANALYSIS AND CHARACTERIZATION

4.1 | Microstructural Analysis

Figure 3 shows the micro-morphologies of G, FG-0.3, FG-0.5, FG-0.8, and FG-1 nanosheets. It can be seen from Figure 3a that graphene G has a flake diameter of approximately 40 μm, presenting a typical lamellar structure with many observable wrinkles. For FG nanosheets, morphologies similar to those of G are observed, with clear wrinkles and layered structures, indicating that the fluorination process does not damage the surface structure of G. Meanwhile, it is observed that the fluorinated graphene layers are exfoliated and the wrinkles are significantly reduced. This is because graphene is attacked by fluorinated gas during high-temperature fluorination, which exfoliates the graphene sheets and thus hinders the mutual stacking of adjacent graphene nanosheets [18]. In fact, as the fluorination degree increases, the average size of fluorinated graphene flakes gradually decreases from 30 μm to 15 μm, a phenomenon that indicates the fluorination process leads to a reduction in the flake size of graphene. Therefore, the exfoliation of FG-1 is more severe than that of FG-0.8, and much more severe than that of FG-0.3 and FG-0.5, which is consistent with their preparation temperatures.

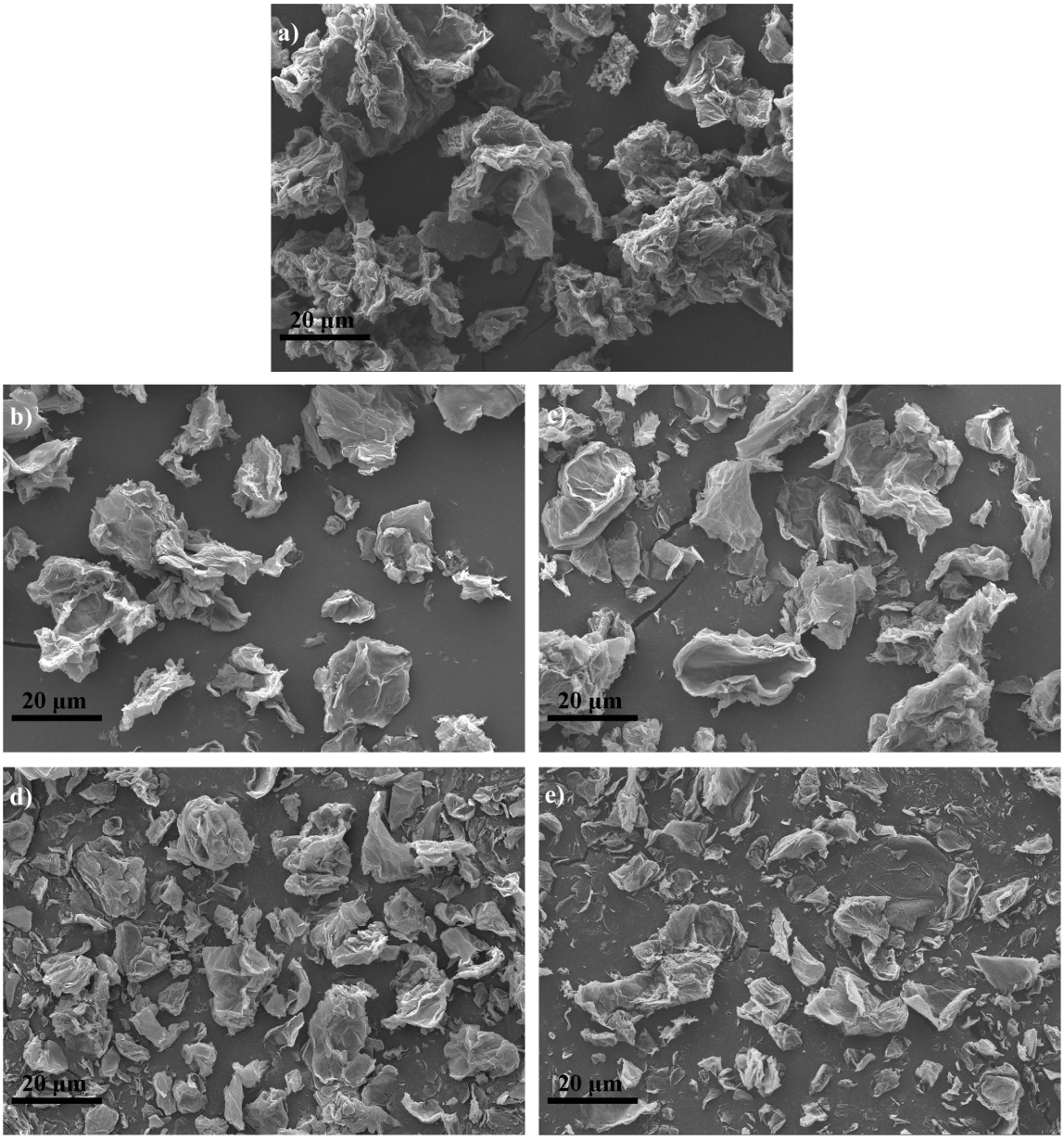

FIGURE 3 SEM images of G and FG sheets: a) G; b) FG-0.3; c) FG-0.5; d) FG-0.8; e) FG-1.

AFM images and thickness curves of G and FG flakes are presented in Figure 4. The average thickness of sample G is approximately 3.327 nm. Given that the thickness of single-layer graphene is 0.335 nm [8], it can be inferred that the graphene in this case has a 10-layer structure. As shown in Figures 4b~e, the thicknesses of FG-0.3, FG-0.5, FG-0.8, and FG-1 are 2.738 nm, 2.611 nm, 2.239 nm, and 2.104 nm, respectively. Based on the reported literature [8], where the interlayer spacing of single-layer FG measured by XRD is 0.783~0.87 nm, it is reasonable to deduce that the number of stacked layers in FG samples ranges from 2 to 4, and this number decreases sequentially with increasing fluorination degree. Overall, these results clearly confirm the few-layer structure of FG flakes.In general, graphene flakes tend to agglomerate severely, but the fluorination process can reduce the stacking size of graphene. As observed in Figure 3, the particle size of FG nanosheets decreases significantly with increasing fluorination level. Furthermore, as fluorination intensifies, the number of stacked layers gradually decreases, which is consistent with previous literature reports [13, 19].

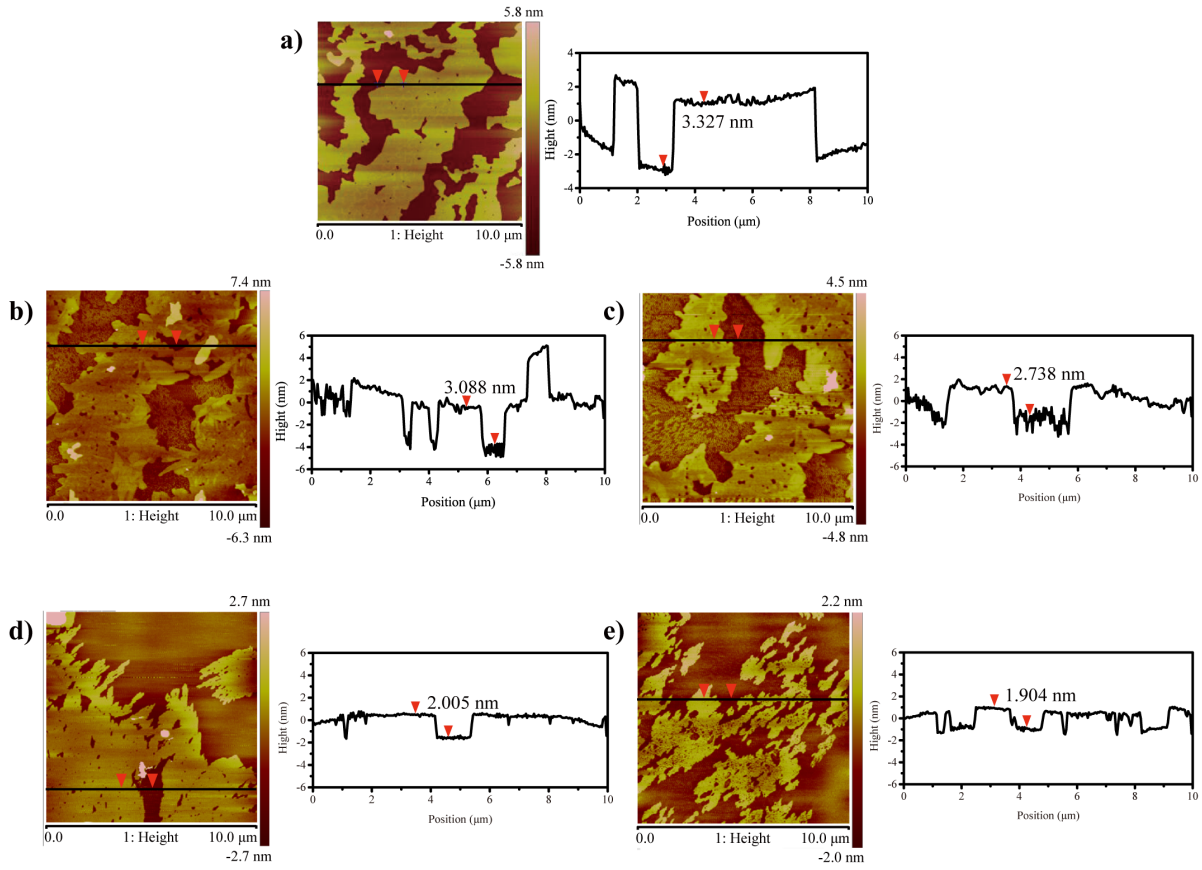

FIGURE 4 AFM images and corresponding thickness curves: a) G; b) FG-0.3; c) FG-0.5; d) FG-0.8 ;e) FG-1.

4.2 | BET Specific Surface Area Analysis

The specific surface area of graphene changes after fluorination treatment to different degrees. Therefore, the BET method was used to analyze the specific surface areas of pristine graphene and the four types of fluorinated graphene. The results are shown that the BET specific surface areas of G, FG-0.3, FG-0.5, FG-0.8, and FG-1 increase sequentially, being 187.62, 199.49, 210.22, 268.16, and 293.78 m^2/g, respectively.

The increase in specific surface area is mainly attributed to the fluorination process reducing the mutual stacking between adjacent graphene nanosheets, which decreases both the flake size and thickness of fluorinated graphene. The relatively small BET specific surface area of graphene is due to its greater thickness, as confirmed by AFM analysis: the thickness of G can reach 10 layers, while the number of stacked layers in fluorinated graphene gradually decreases to 2–4 with increasing fluorination

degree, resulting in the sequential increase in their BET specific surface areas.Consistent with SEM observations, the fluorination process reduces the stacking size of graphene. As the fluorination degree increases, the particle size of fluorinated graphene gradually decreases, which increases the surface area and the number of small pores. Consequently, the pore diameter gradually decreases, while the specific surface area and pore volume increase sequentially.

4.3 | XPS Analysis

X-ray photoelectron spectroscopy (XPS) was employed to further investigate the evolution of elemental composition in graphene and fluorinated graphene with different fluorination degrees by monitoring changes in binding energy (BE). The chemical compositions of the five samples (G, FG-0.3, FG-0.5, FG-0.8, and FG-1) are presented in Table 1. The as-prepared G contains carbon (C) and a small amount of oxygen (O). After fluorination, FG-0.3, FG-0.5, FG-0.8, and FG-1 are primarily composed of C and fluorine (F), with fluorine-to-carbon (F/C) atomic ratios of 0.344, 0.523, 0.808, and 1.045, respectively. Hence, the fluorinated graphene samples are denoted as FG-0.3, FG-0.5, FG-0.8, and FG-1 based on their approximate F/C ratios.

In addition, a small amount of oxygen is present on the surface of these samples due to the existence of oxygen-containing groups. The atomic percentage of oxygen in FG samples is lower than that in G, which is attributed to the replacement of some oxygen atoms by fluorine atoms during the fluorination process.

TABLE 1 Chemical compositions of G and FG measured by XPS.

Samples	C1s (at%)	O1s (at%)	F1s (at%)	F/C
G	96.69	3.31	—	—
FG-0.3	72.12	3.05	24.83	0.344
FG-0.5	64.63	1.60	33.77	0.523
FG-0.8	54.75	1.03	44.22	0.808
FG-1	48.60	0.59	50.81	1.045

The XPS spectra of G, FG-0.3, FG-0.5, FG-0.8, and FG-1 are shown in Figure 5. Two peaks, corresponding to C 1s and F 1s, can be clearly observed in Figure 5a. The intensity of the C 1s peak in the XPS spectrum of FG is lower than that in G. In contrast to G, a new F 1s peak appears in the FG samples, and the intensity of the F 1s peak in FG-0.3, FG-0.5, FG-0.8, and FG-1 gradually increases with the increase in fluorination degree.The high-resolution C 1s spectrum of G is presented in Figure 5c, which can be decomposed into four strong peaks assigned to C=C (sp^2), C-C (sp^3), C-O, and C=O groups, with binding energies at 284 eV, 284.8 eV, 285.4 eV, and 289.2 eV, respectively [16]. Thus, the prepared graphene is a two-dimensional material with a hexagonal honeycomb lattice structure mainly composed of sp^2-hybridized carbon atoms. Due to the presence of some carbon defects and oxygen-containing groups, some carbon atoms transition from sp^2 to sp^3 hybrid orbitals.

After fluorination treatment of graphene, the intensity of the C 1s peak decreases, while the intensity of the F 1s peak increases significantly. The high-resolution C 1s and F 1s spectra of the FG samples are shown in Figures 5b and 5d, respectively. Compared with the high-resolution C 1s spectrum of G, three new peaks appear in the high-resolution C 1s spectrum of FG, namely semi-ionic C-F (BE = 288.2~289.2 eV), covalent C-F (BE = 289.9~290.1 eV), and CF_2 (BE = 290.6~291.3 eV) [20]. In addition, the high-resolution F 1s spectrum can be fitted into the following components: semi-ionic C-F (687.6 eV), covalent C-F (688.5 eV), and CF_2 (689.2 eV) [20, 21, 22]. It can be seen from the figures that FG-0.3 is mainly composed of C=C, C-C, and semi-ionic C-F bonds; FG-0.5 is mainly composed of C=C, C-C, semi-ionic C-F bonds, and covalent C-F bonds; FG-0.8 and FG-1 are mainly composed of covalent C-F bonds and CF_2. Therefore, FG-0.3 and FG-0.5 retain the semi-ionic nature of C-F bonds; the bonding characteristics of C-F bonds in FG-0.5 exhibit both semi-ionic and covalent properties, while FG-0.8 and FG-1 mainly exhibit the covalent characteristics of C-F bonds. It can be observed that as the F doping degree in fluorinated graphene increases, semi-ionic C-F bonds gradually transform into covalent C-F bonds.

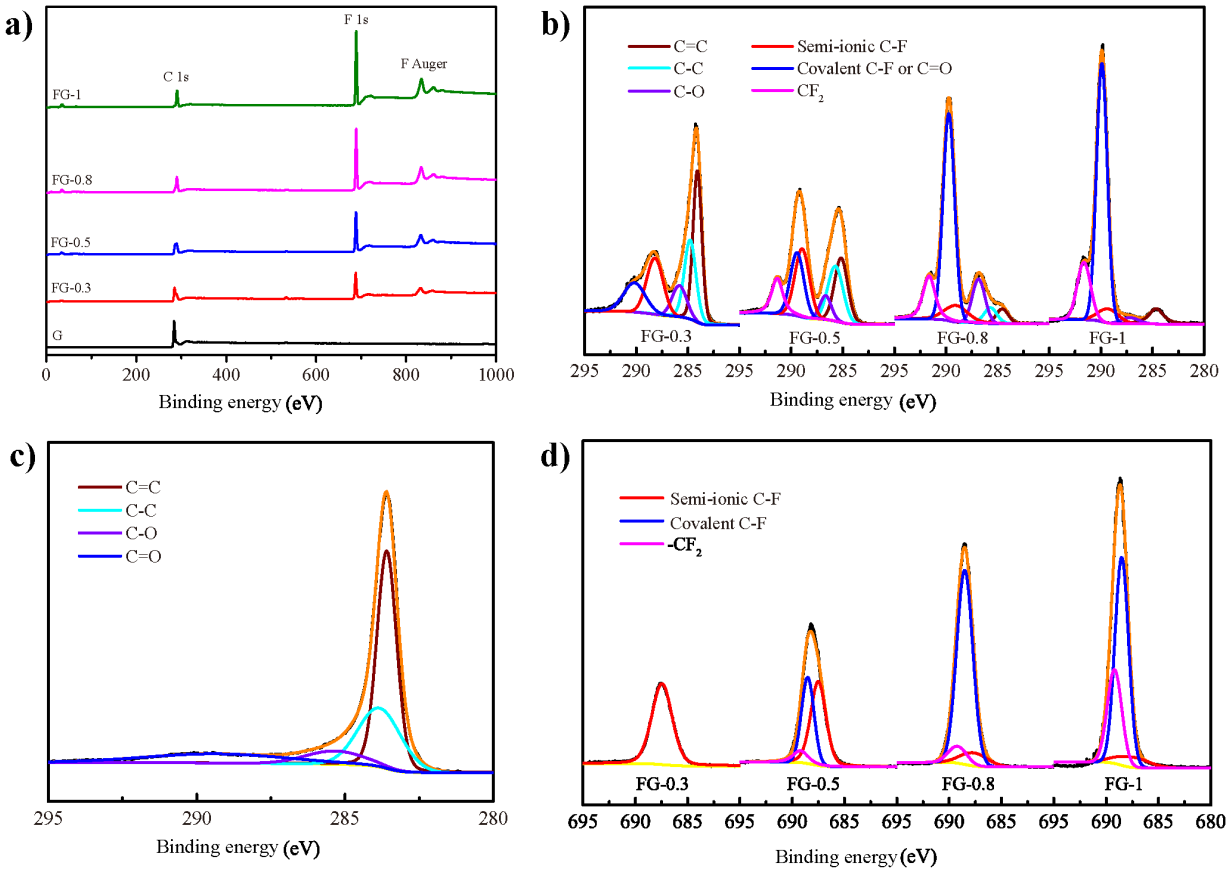

FIGURE 5 XPS survey spectra: a) Survey spectra of G and FG; b) High-resolution C 1s spectra of FG; c) High-resolution C 1s spectrum of G; d) High-resolution F 1s spectra of FG.

Due to the difference in electronegativity between C and F atoms, FG exhibits changes in C-F bonding characteristics (from ionic bonds, semi-ionic bonds to covalent bonds) by controlling the fluorination degree, and this feature results in covalent C-F bonds having stronger electrostatic properties [21, 22]. When fluorine atoms are attached to the carbon atoms in the graphene sheets, these carbon atoms change from sp^2 hybrid orbitals to sp^3 hybrid orbitals. In the case of partially fluorinated materials, when the C atoms on graphene (sp^2 hybridized) are connected to F atoms to form semi-ionic C-F bonds, the planarity of graphene is still maintained, and the semi-ionic C-F bonds show weak covalent characteristics. As the fluorination degree increases, covalent C-F bonds related to the sp^3 hybridization of carbon atoms are formed, and the C-F bonding characteristics transform from semi-ionic to covalent [21, 22]. Since covalent bonds have higher bond energy than semi-ionic bonds, with the increase of fluorination degree, F atoms are bonded more firmly to the graphene sheet structure. Therefore, the chemical stability of FG-0.3, FG-0.5, FG-0.8, and FG-1 gradually increases.

4.4 | Thermogravimetric Analysis

To verify the influence of the nature of C-F bonds on the chemical stability of materials, thermogravimetric analysis (TGA) was performed on graphene G and fluorinated graphene FG-0.3, FG-0.5, FG-0.8, and FG-1 up to 800 °C. Figure 6 shows the thermogravimetric curves of the five powders in a nitrogen atmosphere. The mass loss of G powder in the temperature range of 30–100 °C is due to the evaporation of physically adsorbed water upon heating. There is only approximately 4.7% weight loss in the range of 100–700 °C, which is attributed to the decomposition of oxygen-containing groups. In the temperature range of 700–800 °C, the weight loss is about 7.6%, mainly caused by carbon defects on the graphene sheets. Therefore, the strong covalent bonding between carbon atoms renders the graphene structure highly stable.

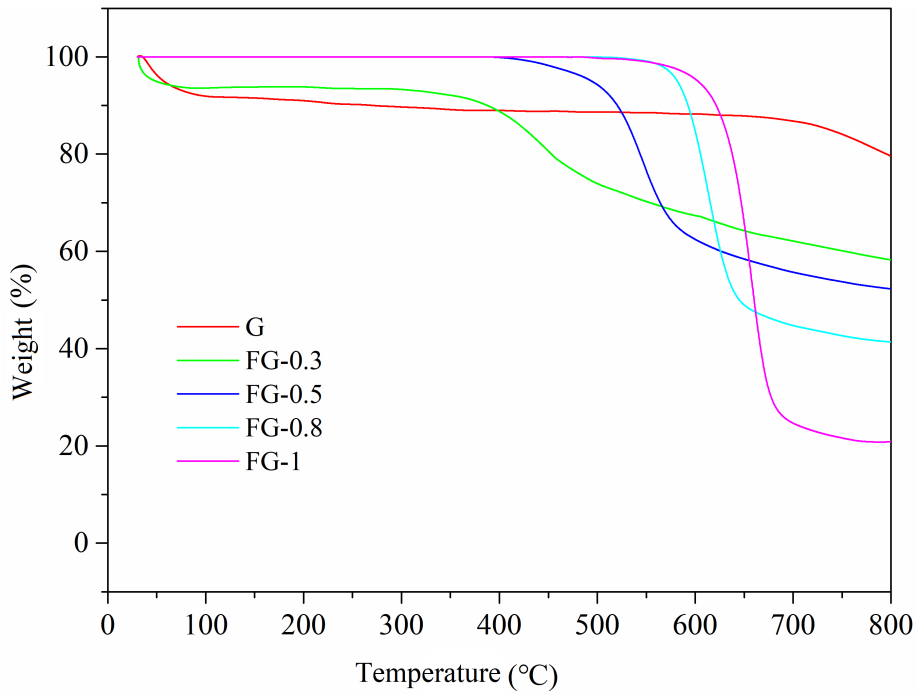

FIGURE 6 TG curves of G and FG.

However, the thermal stability of FG, obtained by fluorinating G, is significantly lower than that of G. As can be seen from the figure, the mass loss of FG-0.3 in the temperature range of 30–100 °C is caused by the evaporation of physically adsorbed water molecules. The FG-0.3 sample starts to decompose at 374.2 °C, and the mass loss is attributed to the decomposition of oxygen-containing groups, the breaking of unstable C-C bonds, and some semi-ionic C-F bonds. The decomposition temperatures of FG-0.5, FG-0.8, and FG-1 increase sequentially from 440.5 °C and 552.4 °C to 579.3 °C. According to theoretical calculation results [23], the characteristics of C-F bonds depend on the degree of fluorination. Compared with ionic C-F and semi-ionic C-F bonds, covalent C-F bonds have shorter bond lengths and higher bond energies, making them more stable. With the increase in fluorination degree, the bonding of F atoms on graphene nanosheets becomes stronger, and the covalent CF_2 and C-F bonds on the surface are more resistant to thermal decomposition than semi-ionic C-F bonds, thus leading to a gradual increase in the thermal decomposition temperature of FG.

The weight loss rates of FG-0.3, FG-0.5, FG-0.8, and FG-1 are 43.1%, 47.7%, 58.6%, and 79.1%, respectively, which is attributed to the detachment of fluorine atoms with different concentrations from the graphene sheets, resulting in partial reduction of the prepared fluorinated graphene. Moreover, the weight loss rate increases with the increase in F doping degree, indicating a gradual increase in fluorine content in FG-0.3, FG-0.5, FG-0.8, and FG-1, which is consistent with the previous XPS analysis results.

5 | CONCLUSION

In this study, graphene was prepared from natural flake graphite via secondary chemical intercalation, microwave expansion, and liquid-phase reduction. Subsequently, fluorinated graphene with fluorine-to-carbon (F/C) ratios of 0.344, 0.523, 0.808, and 1.045 (denoted as FG-0.3, FG-0.5, FG-0.8, and FG-1, respectively) was synthesized at different temperatures using the direct gas fluorination method.

The micro-morphology, chemical composition, and thermal stability of the five nanoscale fillers were characterized by SEM, AFM, BET, XPS, and TG techniques. It was found that both G and FG exhibit clear wrinkled and layered structures. With the increase in fluorination degree, the average particle size and number of layers of fluorinated graphene flakes gradually decrease, leading to a sequential increase in the BET specific surface areas of G, FG-0.3, FG-0.5, FG-0.8, and FG-1. The transition from

semi-ionic C-F bonds to covalent C-F bonds and CF_2 bonds between C and F atoms enhances the binding of F atoms to the graphene sheet structure. Consequently, the thermal decomposition temperatures and weight loss rates of FG-0.3, FG-0.5, FG-0.8, and FG-1 increase sequentially with the increasing fluorination degree.

CONFLICT OF INTEREST

The authors do not have any possible conflicts of interest.

FUNDING

This study was funded by Science and Technology Project of Hebei Education Department (No. BJK2023030) , S&T Program of Qinhuangdao (No. 202301A367) and Doctoral Foundation of Hebei University of Environmental Engineering (2023BSJJ06).

REFERENCES

[1] Gou Z, Xi W, Jiang W, Zhang Z, Zhao J, Zhou J, et al. Study on the dielectric properties of fluorinated graphene. FlatChem 2025;51:100862.
[2] Ci X, Zhao W, Luo J, Wu Y, Ge T, Xue Q, et al. How the fluorographene replaced graphene as nanoadditive for improving tribological performances of GTL-8 based lubricant oil. Friction 2021;9(3):488–501.
[3] Yongzhen S, Hanlu Z, Yelin S, Jingjuan J. Dynamic Coupling Analysis of High-Speed Railway and Remote Investment Network in China. Tropical Geography 2024;44(7).
[4] Hao B, Y W, Xu X, Guo J. Review of AUV Underwater Recovery Docking Studies. International Journal of Applied Mathematics in Control Engineering 2024;7(1):41–47.
[5] Cui J, Ma H, Gong S, Wang D, Zhang S, Liu Z, et al. Water-dispersible fluorinated graphene/MXene with stable heterostructure for responsive lubrication and long-term anticorrosion. Tribology International 2025;p. 110850.
[6] Xue Z, Lv D, Du Y, Huo D. Digital Twin of Permanent Magnet Synchronous Motor Based on Finite Element Analysis and UNITY. International Journal of Applied Mathematics in Control Engineering 2024;7(2):156–164.
[7] Nair RR, Ren W, Jalil R, Riaz I, Kravets VG, Britnell L, et al. Fluorographene: a two-dimensional counterpart of Teflon. small 2010;6(24):2877–2884.
[8] Zbořil R, Karlickỳ F, Bourlinos AB, Steriotis TA, Stubos AK, Georgakilas V, et al. Graphene fluoride: a stable stoichiometric graphene derivative and its chemical conversion to graphene. small 2010;6(24):2885–2891.
[9] Yan X, Zhang X, Lv B, Zou Y, Zhang M, We H, et al. Atmospheric Switching between Etching and High-Quality Fluorination of Graphene by XeF2. ACS Applied Materials & Interfaces 2025;17(21):31257–31264.
[10] Liang L, Song L, Yang Y, Li F, Ma Y. Tribological properties of polytetrafluoroethylene improved by incorporation of fluorinated graphene with various fluorine/carbon ratios under dry sliding condition. Tribology Letters 2021;69(1):21.
[11] Jahanshahi M, Kowsari E, Haddadi-Asl V, Khoobi M, Bazri B, Aryafard M, et al. An innovative and eco-friendly modality for synthesis of highly fluorinated graphene by an acidic ionic liquid: Making of an efficacious vehicle for anti-cancer drug delivery. Applied Surface Science 2020;515:146071.
[12] Xu JY, Yu JS, Liao JH, Yang XB, Wu CY, Wang Y, et al. Opening the band gap of graphene via fluorination for high-performance dual-mode photodetector application. ACS applied materials & interfaces 2019;11(24):21702–21710.
[13] Wang X, Dai Y, Gao J, Huang J, Li B, Fan C, et al. High-yield production of highly fluorinated graphene by direct heating fluorination of graphene-oxide. ACS applied materials & interfaces 2013;5(17):8294–8299.
[14] Wang D, Jia X, Yang J, Wang Z, Song H. Fluorinated graphene intercalated by carbon quantum dots: Triple effect for reducing friction and wear. Chemical Engineering Journal 2025;512:162393.
[15] Tian R, Jia X, Yang J, Li Y, Song H. Large-scale, green, and high-efficiency exfoliation and noncovalent functionalization of fluorinated graphene by ionic liquid crystal. Chemical Engineering Journal 2020;395:125104.
[16] Wu Y, Zhao W, Qiang Y, Chen Z, Wang L, Gao X, et al. π-π interaction between fluorinated reduced graphene oxide and acridizinium ionic liquid: Synthesis and anti-corrosion application. Carbon 2020;159:292–302.
[17] Wang D, Jia X, Tian R, Yang J, Su Y, Song H. Tuning fluorine content of fluorinated graphene by an ionothermal synthesis method for achieving excellent tribological behaviors. Carbon 2024;218:118649.
[18] Sun L, Wang L, Tian C, Tan T, Xie Y, Shi K, et al. Nitrogen-doped graphene with high nitrogen level via a one-step hydrothermal reaction of graphene oxide with urea for superior capacitive energy storage. Rsc Advances 2012;2(10):4498–4506.
[19] Li W, Zhao W, Mao L, Zhou S, Liu C, Fang Z, et al. Investigating the fluorination degree of FG nanosheets on the tribological properties of FG/PI composite coatings. Progress in Organic Coatings 2020;139:105481.
[20] Sato Y, Itoh K, Hagiwara R, Fukunaga T, Ito Y. On the so-called "semi-ionic" C–F bond character in fluorine–GIC. Carbon 2004;42(15):3243–3249.
[21] Zhou S, Sherpa SD, Hess DW, Bongiorno A. Chemical bonding of partially fluorinated graphene. The Journal of Physical Chemistry C 2014;118(45):26402–26408.
[22] Lee JH, Koon GKW, Shin DW, Fedorov V, Choi JY, Yoo JB, et al. Property Control of Graphene by Employing "Semi-Ionic" Liquid Fluorination. Advanced Functional Materials 2013;23(26):3329–3334.
[23] Feng W, Long P, Feng Y, Li Y. Two-dimensional fluorinated graphene: synthesis, structures, properties and applications. Advanced Science 2016;3(7):1500413.

Lifen Liang currently works at Hebei University of Environmental Engineering in Qinhuangdao, China. She obtained her doctoral degree from Yanshan University in Qinhuangdao, China in 2022. Her main research interests include nano-tribology, research on self-lubricating composite materials, and engineering design of environmental protection equipment.

Xiurong Sun currently works at Hebei University of Environmental Engineering, Qinhuangdao, China. She obtained her MS degree from Yanshan University, China in 2010 and her PhD degree from Yanshan University, China in 2019. Her main research interests are in the areas of rod string dynamics and rod-tubing wear.

Longjie Miao is currently pursuing a bachelor's degree in the Department of Environmental Engineering at Hebei University of Environmental Engineering in Qinhuangdao. His main research directions are the design of environmental protection equipment and the preparation of engineering materials.

Shenghang Ma is currently pursuing his bachelor's degree in Environmental Protection Equipment Engineering at Hebei University of Environmental Engineering, Qinhuangdao, China. His main research interests focus on the design of environmental protection equipment and the preparation of engineering materials.